

# Modification of Enzyme Activity by Vibrational Strong Coupling of Water

Robrecht M. A. Vergauwe, Anoop Thomas, Kalaivanan Nagarajan, Atef Shalabney, Jino George, Thibault Chervy, Marcus Seidel, Eloïse Devaux, Vladimir Torbeev,\* and Thomas W. Ebbesen\*

**Abstract:** Vibrational strong coupling (VSC) has recently emerged as a completely new tool for influencing chemical reactivity. It harnesses electromagnetic vacuum fluctuations through the creation of hybrid states of light and matter, called polaritonic states, in an optical cavity resonant to a molecular absorption band. Here, we investigate the effect of vibrational strong coupling of water on the enzymatic activity of pepsin, where a water molecule is directly involved in the enzyme's chemical mechanism. We observe an approximately 4.5-fold decrease of the apparent second-order rate constant  $k_{cat}/K_m$  when coupling the water stretching vibration, whereas no effect was detected for the strong coupling of the bending vibration. The possibility of modifying enzymatic activity by coupling water demonstrates the potential of VSC as a new tool to study biochemical reactivity.

Vibrational strong coupling entails the formation of hybrid light-matter states, or polaritonic states, by placing a molecular species in a photonic cavity resonant to one of its vibrational absorption bands under the right conditions (Figure 1A).<sup>[1–5]</sup> A resonant cavity is a structure which confines light spatially at well-defined frequencies, for

example, two parallel mirrors facing each other form a Fabry–Perot cavity (Figure 1B and Supporting Information,

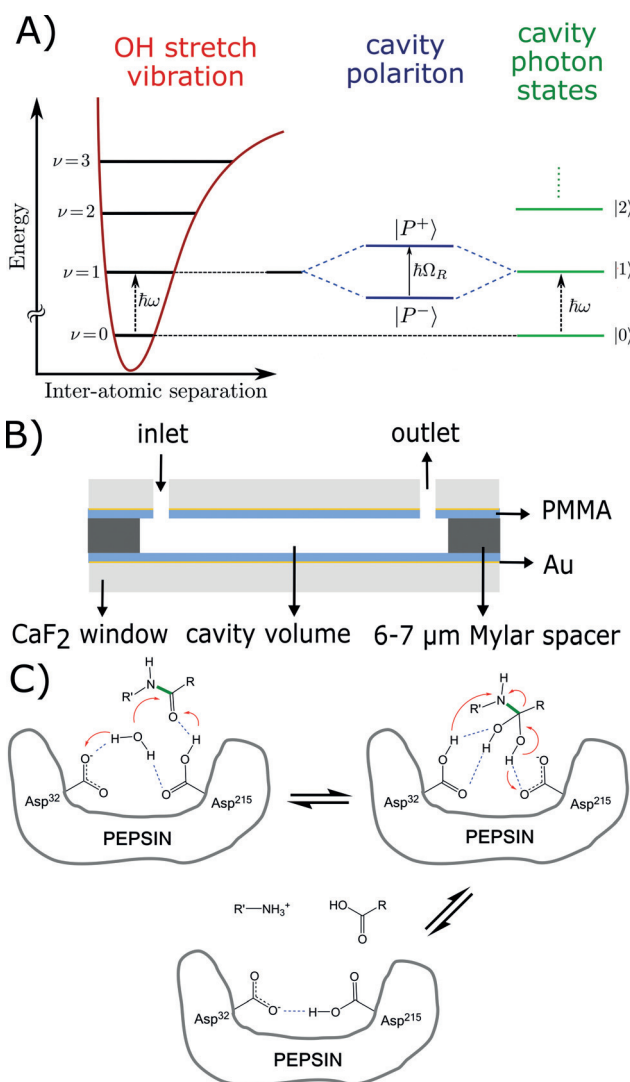


**Figure 1.** Vibration strong coupling and pepsin. A) Schematic outline of strong light–matter interaction with molecular vibrations. In an on resonance cavity where  $\hbar\omega_{\text{vibr}} = \hbar\omega_{\text{cavity}}$ , the ground and first excited state of a vibration will combine with the photon number state of the photonic cavity to produce two new polariton states,  $P^+$  and  $P^-$ , separated by the vacuum Rabi splitting  $\hbar\Omega_R$ . B) Schematic drawing of the microfluidic cavities used here for studying pepsin-mediated peptide hydrolysis under VSC of the water mid-infrared bands. C) Mechanistic model of peptide bond cleavage in the active site of pepsin based on ref. [8].

[\*] Dr. R. M. A. Vergauwe, Dr. A. Thomas, Dr. K. Nagarajan, Dr. J. George, Dr. T. Chervy, Dr. M. Seidel, Dr. E. Devaux, Dr. V. Torbeev, Prof. T. W. Ebbesen  
University of Strasbourg, CNRS, ISIS & icFRC  
8 allée Gaspard Monge, 67000 Strasbourg (France)  
E-mail: torbeev@unistra.fr  
ebbesen@unistra.fr

Dr. A. Shalabney  
Braude College, Snunit Street 51, Karmiel 2161002 (Israel)

Dr. J. George  
Present address: Department of Chemical Sciences,  
Indian Institute of Science Education and Research Mohali  
Knowledge city, Sector 81, SAS Nagar, Manauli  
PO 140306 Mohali (India)

Dr. T. Chervy  
Present address: Institute for Quantum Electronics, ETH Zurich  
Otto-Stern-Weg 1, 8093 Zurich (Switzerland)

Supporting information, including the materials and methods, and the ORCID identification number(s) for the author(s) of this article can be found under:

<https://doi.org/10.1002/anie.201908876>.

© 2019 The Authors. Published by Wiley-VCH Verlag GmbH & Co. KGaA. This is an open access article under the terms of the Creative Commons Attribution Non-Commercial NoDerivs License, which permits use and distribution in any medium, provided the original work is properly cited, the use is non-commercial, and no modifications or adaptations are made.

Figure S1). The resulting polaritonic states are collective, involving all the molecules coupled to the resonant cavity mode. In the absorption spectrum, the emergence of strong coupling is manifested by the splitting of the molecular absorption and cavity peak into two new polariton peaks, conventionally denoted P+ and P−, separated at resonance by the vacuum Rabi splitting  $\hbar\Omega_R$  (Figure 1 A). To enter the strong coupling regime, the molecular vibration and cavity need to exchange energy between them at a rate that corresponds to the Rabi frequency  $\Omega_R$ , which exceeds the rate of losses in the system. This can be met for molecules with strong infrared transitions at high concentrations inside a cavity. For a recent perspective oriented towards molecular and material science, the reader is referred to ref. [3]. For a further discussion of the physics of quantum strong light–matter interaction, please see refs. [7].

Although the phenomenon and the theory of strong light–matter coupling has been explored for several decades,<sup>[3,7]</sup> the idea that this could influence material properties was only very recently realized.<sup>[1,2,5]</sup> Vibrational strong coupling can be utilized to slow down or speed up organic reactions and even alter the yield ratio of two competing deprotection reactions on a given molecule.<sup>[1]</sup> More importantly, because the formation of polaritonic states involves the zero-point energies of the cavity and the vibrational transition, it occurs even in the dark.<sup>[3,7]</sup> This makes it very distinct from traditional photochemistry or previous work in mode-selective chemistry with infrared lasers.<sup>[9]</sup>

The modification of properties under strong light–matter interactions is not limited to non-biological samples. It is entirely possible to couple biological chromophores<sup>[10]</sup> or vibrations of proteins<sup>[6]</sup> to Fabry–Perot cavities. However, functional consequences or biologically relevant applications have not been reported so far. Here, we present the effects of vibrational strong coupling of the liquid-water environment via its two absorption bands in the mid-infrared on the enzyme pepsin and show that VSC of the stretching modes of water slows down its proteolytic activity. Pepsin ( $M_w = 35$  kDa) is a digestive protease that has long served as a model for the class of aspartic proteases.<sup>[8]</sup> Its catalytic mechanism rests on the presence of a pair of essential aspartic acid residues in the active site that work in a concerted way to activate a water molecule as a nucleophile for attack on the carbonyl carbon of a scissile amide bond (Figure 1 C).<sup>[8]</sup> From a kinetic perspective, pepsin can be described by a simple Michaelis–Menten model: a single substrate-binding step followed by a single chemical step.

The choice to strongly couple the water OH stretching modes was motivated by several reasons. Although the amide I band of a protein can be strongly coupled,<sup>[6]</sup> measuring enzyme activity with either the substrate or the enzyme strongly coupled is extremely impractical. It would require either of these species to be present at concentrations in the high mM range at least.<sup>[1]</sup> Instead, we decided to strongly couple water, which has two prominent absorption peaks in the IR, namely the broad OH stretching absorption band centered around  $3367\text{ cm}^{-1}$  and the bending mode at  $1642\text{ cm}^{-1}$ .<sup>[11,12]</sup> Because water plays the dual role of reactant (pepsin is a hydrolase)<sup>[7]</sup> and a medium needed for the correct

folding and function of pepsin,<sup>[10–14]</sup> it is very intriguing to see the effects of VSC of water on enzyme activity.

We first demonstrate the strong coupling of water as shown in Figure 2. We chose to use the final solution with the complete reaction mixture to be in the exact conditions of the

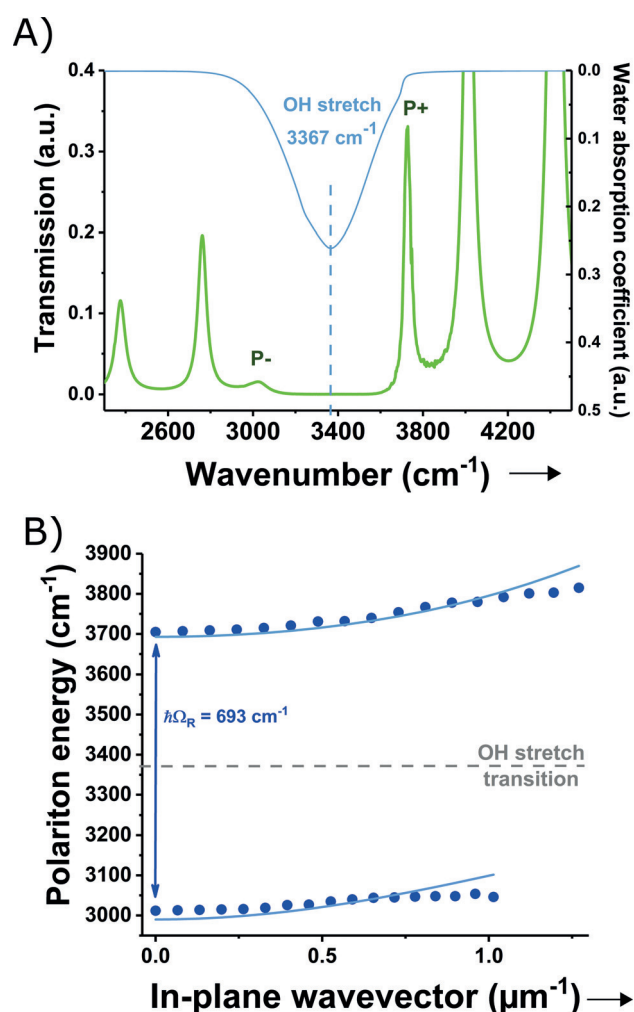


**Figure 2.** Vibrational strong coupling of the water OH stretching mode. A) Infrared transmission spectrum of a cavity containing a reaction mixture with pepsin and on-resonance at normal incidence. Overlay with the water absorption coefficient (i.e. the imaginary part of the complex refractive index; light blue curve). B) Angle-dependent dispersion measurement. The cavity was tuned to resonance at  $0^\circ$  or  $k_{\parallel} = 0$  with measured vacuum Rabi splitting of  $693\text{ cm}^{-1}$ . Circles: measured upper and lower polariton energies. Line: fit with a coupled oscillator model including the anti-resonant and dipolar self-energy terms.<sup>[15]</sup>

kinetic experiments to follow. Figure 2 illustrates the case when we target the OH stretching peak at  $3367\text{ cm}^{-1}$  (FWHM =  $409\text{ cm}^{-1}$ ). This is a composite peak of the symmetric and antisymmetric stretching modes of water inhomogeneously broadened by H-bonding. It should be noted that the solutes (buffer, enzyme, and substrate) are not visible in the IR spectrum due to their low concentrations (see Figure S1 D in the Supporting Information for the total IR

absorption spectrum). As in earlier work on chemical reactivity, the cavity is constructed with two Au mirrors on CaF<sub>2</sub> windows coated with a thin PMMA (polymethylmethacrylate) layer and separated with approximately 7  $\mu\text{m}$  thick Mylar spacer in a commercial IR transmission cell assembly (Supporting Information, Figure S1 A,B). The PMMA layers serve to insulate the Au mirrors from any chemical effects. As expected, the transmission spectrum of the empty cavity consists of series of regularly spaced peaks separated by a free spectral range of 595 to 680  $\text{cm}^{-1}$  (Supporting Information, Figure S1 C). After injecting the reaction mixture, the spectral signature of the strong coupling of OH stretching band at normal incidence becomes apparent as shown in Figure 2 A. The spectral region of the stretching vibration now comprises a gap flanked by two new polaritonic peaks, noticeably sharper than the original cavity modes and the bare absorption band. The P- peak has a lower intensity compared the P + peak because of the higher absorption of water and Au in the P- region (the water stretching band is slightly asymmetric).<sup>[11]</sup> To characterize the cavities, we extrapolate the coupled cavity mode position from one of the uncoupled cavity modes in the 5700–6300  $\text{cm}^{-1}$  region (typical the 12th order mode) where water shows no absorption bands. Examining further the angle-dependent dispersion and cavity detuning behaviour of our system (Figure 2 C and Supporting Information, Figure S2), we note in both cases the typical signature of strong coupling: dispersion of both upper and lower polariton branches with anti-crossing at the bare absorption peak position. It is important to note that the kinetic data, presented further down, is collected for cavities tuned at normal incidence.

The vacuum Rabi splitting of the on-resonance cavity shown in Figure 2 A is 703  $\text{cm}^{-1}$  or about 21 % of the bare transition energy. The fact that this value is larger than either the OH stretching (FWHM = 409  $\text{cm}^{-1}$ ) or cavity mode (FWHM = 50–55  $\text{cm}^{-1}$ ) linewidths constitutes further evidence for a strong light–matter interaction. The high value of vacuum Rabi splitting relative to bare OH stretch transition energy indicates that the system is in the ultra-strong coupling regime (USC). The value found here is similar to earlier work on USC of Fe(CO)<sub>5</sub> and CS<sub>2</sub> where the vacuum Rabi splittings to the bare transition energies were 24 and 19 %, respectively.<sup>[15]</sup> In this regime, which arises when the vacuum Rabi splitting amounts to a noticeable fraction of the coupled transition energy, the theoretical description based on the Jaynes–Cummings Hamiltonian with the rotating-wave approximation becomes insufficient because contributions from the anti-resonant terms and dipolar self-energy become non-negligible.<sup>[15,16]</sup> Here, fitting the polaritonic detuning branches (Supporting Information, Figure S2) with the coupled oscillator models for both the strong and ultra-strong coupling results in a slightly better fit for the model for USC (evident from a roughly 30 % lower sum of squared residuals). From the asymptotic convergence of the two modelled polariton branches, we derive a value of 28  $\text{cm}^{-1}$  for the vibrational polaritonic band gap. Furthermore, the polaritonic peaks are narrower than the cavity mode (36  $\text{cm}^{-1}$  vs. 55  $\text{cm}^{-1}$  for the example in Figure 2 A)

indicating again that the system is in a non-Markovian regime.<sup>[15,16]</sup>

To assay the enzymatic activity of the pepsin under VSC, a profluorescent substrate S was designed and synthesised based on a 11-residue peptide with a FRET pair consisting of ATTO488 and ATTO532 and N- and C-terminal PEG arms (structure given in Figure S3 A in the Supporting Information).<sup>[17]</sup> The two main pepsin cleavage sites appear to be Leu-4/Ser-5 and Ser-5/Arg-6 (Supporting Information, Figure S4 D,E) from the mass spectrometry analysis. The steady-state parameters  $k_{\text{cat}}$  and  $K_{\text{m}}$  were estimated  $45 \pm 11 \text{ min}^{-1}$  and  $208 \pm 81 \mu\text{M}$ , respectively, (Supporting Information, Figure S4 C) outside the cavity. This reaction can be monitored by time-based fluorescence measurements as digestion lifts the quenching of ATTO488 restoring its emission around 520 nm (Supporting Information, Figure S4 A,B).

Figure 3 B displays two examples of product concentration traces measured with an initial substrate concentration of 0.4  $\mu\text{M}$  in different conditions. The blue and green curve represent data measured in cavities for off- and on-resonance, respectively, with the water OH stretching band. Reaction progress in the on-resonant cavity is clearly slower than the

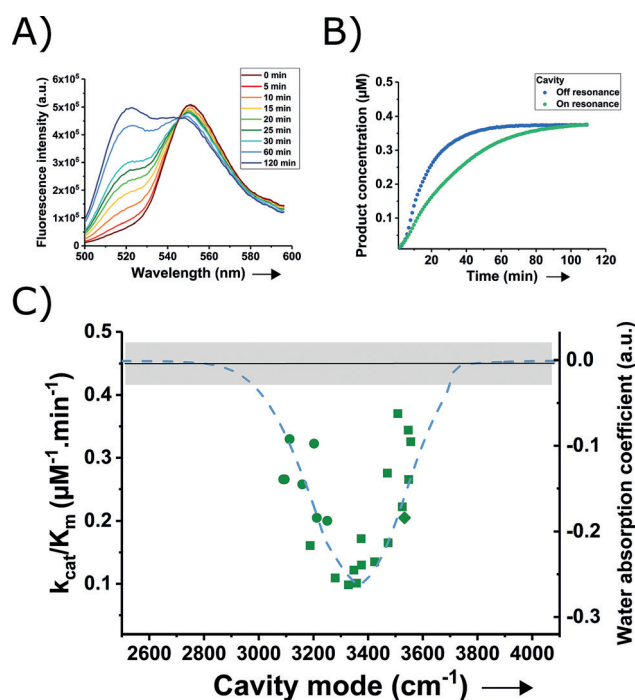


**Figure 3.** Pepsin enzymatic activity under vibrational strong coupling of the water stretching mode. A) Example of a ratiometric measurement of pepsin hydrolytic activity towards substrate S in a Fabry–Perot cavity. Emission spectra between 500–596 nm were repeatedly collected under excitation with 485 nm light. B) Two examples of the product concentration time traces on- and off-resonance to the water stretching vibration. C) Detuning curve of the initial velocities of S digestion. Green circles: 6th order mode coupled. Green squares: 7th order mode coupled. Green diamond: 10th order mode coupled. Blue dashed curve: water absorption coefficient. Black line: average measured initial reaction velocity of reactions measured in a cell. Gray area: mean  $\pm$  standard deviation of measurements in a cell.

off-resonance case. These examples illustrate the general trend we observe when executing the pepsin-catalysed digestion of S in cavities tuned across the OH stretching transition. Figure 3C displays the measured apparent second-order rate constants  $k_{\text{cat}}/K_{\text{m}}$  as a function of the position of the cavity mode closest to the coupled water band (predominantly the 6th or 7th order mode). The thicknesses of available spacers restrict us to scanning the OH vibration from 3200 to 3550  $\text{cm}^{-1}$ . In the absence of cavity effects, that is, when observed in a cell, the observed rate constant is  $0.450 \pm 0.038 \mu\text{M min}^{-1}$  (mean  $\pm$  standard deviation; denoted in Figure 3C as a black line in a gray area). The rate constant reduces to about  $0.100 \mu\text{M min}^{-1}$  for on-resonance cavities tuned to the maximum of the water OH stretching band. This represents a nearly 4.5-fold reduction in the apparent second order rate constant  $k_{\text{cat}}/K_{\text{m}}$ . The detuning dependency essentially follows the shape of the water OH band as can be noted from the overlay of the measured data and the water absorption coefficient (i.e. the imaginary part of the complex refractive index) in Figure 3C. Overall, the cavity tuning response demonstrates the effect of strong coupling the water OH stretching band on the proteolytic activity of pepsin.

The findings reported here are consistent with the fact that coupling a vibrational mode to a photonic cavity alters the potential energy landscape causing modifications of ground-state reactivity.<sup>[1,2,5]</sup> However, there are still two possible scenarios for the modification of the enzymatic activity. One is the direct modification of the chemistry in the active site and the other the perturbation of the tertiary structure of the enzyme. Both scenarios might be present simultaneously and competing, giving rise to the overall observed effect.

Given the previous work of our group and of others,<sup>[1,4]</sup> it can be argued that the chemical step, involving the nucleophilic attack of the water molecule hydrogen-bonded in the active site (Figure 1B), is altered. For this not to be the case, the vibrational transition energies of this water molecule would need to be shifted to values beyond the polaritonic gap region, that is, less than 3000  $\text{cm}^{-1}$  or greater than 3700  $\text{cm}^{-1}$ , in order to be completely decoupled from those of the bulk water. Such shifts seem unreasonably large judging by the literature on anion water solvation.<sup>[18]</sup> Unfortunately, quantum mechanical/molecular dynamics studies on aspartic proteases do not address this question directly (see ref. [19] and references therein).

On the other hand, the proper function of pepsin depends on its folding as a globular protein and substrate binding/product release in its natural and necessary environment, namely water.<sup>[11,14]</sup> VSC of water could potentially affect the balance of intermolecular forces, such as hydrogen bonding, van der Waals interactions, and hydrophobic interactions, governing these equilibria.<sup>[11,13]</sup> Alterations of this kind would automatically lead to changes in the observed values of  $k_{\text{cat}}$  and  $K_{\text{m}}$  as the enzyme conformational distribution/dynamics and enzyme-substrate/product interactions would all be modified. It is worth bearing in mind that relatively small Gibbs free energy differences are involved here,<sup>[14]</sup> meaning that a small energy change could have noticeable consequences on observable equilibria and kinetics.

One could expect that there is also an effect from strongly coupling the OH bending band at 1642  $\text{cm}^{-1}$ . For the current cavity configuration and reaction buffer, bringing a cavity mode in resonance leads to a vacuum Rabi splitting of about 164  $\text{cm}^{-1}$  or 10% of the bare transition energy (Supporting Information, Figure S5). This value exceeds both the line-width of the bare transition and of typical cavity mode (91  $\text{cm}^{-1}$  and 31  $\text{cm}^{-1}$ , respectively). The lower value is essentially due to the lower oscillator strength of the bending vibration compared to the stretching vibration as the Rabi splitting is also the dipole interaction energy between matter and cavity field (in the Jaynes–Cumming model).<sup>[3–5]</sup> The characteristic dispersive behaviour of both polariton branches can be readily observed in both cavity-length and angle-dependent detuning experiments. Nevertheless, no effect from coupling this mode could be detected in the kinetic data (see the Supporting Information). The large difference in response between the stretching and bending vibration is not something intrinsic to the VSC of these bands and probably points to mechanistic aspects of pepsin hydrolysis not yet fully understood. However, given the spread of measured initial digestion rates, a small effect might still be present but not resolvable. Previous work on VSC modifications of organic reactions also shows that the rate constants depend on the vacuum Rabi splitting in a non-linear, typically an exponential way.<sup>[1,2]</sup> If this is the case for the proteolytic reaction studied here, then it could contribute to making the effect of the VSC of the bending mode undetectable. In our case, the vacuum Rabi splitting for the bending mode is significantly smaller than for the stretching mode (i.e. 164  $\text{cm}^{-1}$  or 10% of the bare transition energy of bending vibration versus approximately 700  $\text{cm}^{-1}$  or 21% of the bare transition energy of stretching vibration, respectively). Nevertheless, in previous measurements of chemical reactions under VSC, clear effects were observed while attaining vacuum Rabi splitting between 5 and 10% of the bare transition energy.<sup>[1]</sup> It is important to point out that, similarly, only a subset of vibrational modes was found to perturb the reactions rates under VSC of organic molecules.<sup>[1,2]</sup>

In conclusion, we have succeeded in modifying the rate of an enzymatic hydrolysis reaction under strong coupling of the water vibrations. This presents us with a completely novel and generic tool for altering the potential energy landscape of biological entities such as proteins and nucleic acid, as water is vital for the proper functioning of almost any biological molecule. This opens up new avenues in studying biological hydration and its consequences on conformational dynamics and enzymatic performance,<sup>[11]</sup> or vibrational dynamics and energy flow relevant for (bio)chemical reactivity.<sup>[20]</sup> While the details of the mechanism of VSC on molecular systems are not yet fully understood, further investigations on simpler models, both experimental and theoretical,<sup>[5,21]</sup> will provide more insight. Consideration of the structure–function relationships and reaction mechanisms at play in such system will be critical to unveil all the subtle effects of VSC on biomolecules. Finally, examining other enzymes and targeting intrinsic protein vibrations using the cooperative effect might uncover different effects (for example, activity enhance-

ments) as already seen for other chemical reactions under VSC.<sup>[1,2]</sup>

## Acknowledgements

We wish to thank Régis Boehringer, Aromal Asokan, and Elise Naudin for assistance during the synthesis of the substrate. The authors acknowledge support of the International Center for Frontier Research in Chemistry (icFRC, Strasbourg), the ANR Equipex Union (ANR-10-EQPX-52-01), the Labex NIE projects (ANR-11-LABX-0058 NIE), and CSC (ANR-10-LABX-0026 CSC) within the Investissement d'Avenir program ANR-10-IDEX-0002-02 and the ERC (project no 788482 MOLUSC).

## Conflict of interest

The authors declare no conflict of interest.

**Keywords:** enzymes · light-matter strong coupling · optical cavities · vibrational spectroscopy · water

**How to cite:** *Angew. Chem. Int. Ed.* **2019**, *58*, 15324–15328  
*Angew. Chem.* **2019**, *131*, 15468–15472

- [1] a) A. Thomas, J. George, A. Shalabney, M. Dryzhakov, S. J. Varma, J. Moran, T. Chervy, X. Zhong, E. Devaux, C. Genet, et al., *Angew. Chem. Int. Ed.* **2016**, *55*, 11462–11466; *Angew. Chem.* **2016**, *128*, 11634–11638; b) A. Thomas, L. Lethuillier-Karl, K. Nagarajan, R. M. A. Vergauwe, J. George, T. Chervy, A. Shalabney, E. Devaux, C. Genet, J. Moran, et al., *Science* **2019**, *363*, 615–619; c) J. Lather, P. Bhatt, A. Thomas, T. W. Ebbesen, J. George, *Angew. Chem. Int. Ed.* **2019**, *58*, 10635–10638; *Angew. Chem.* **2019**, *131*, 10745–10748.
- [2] H. Hiura, A. Shalabney, J. George, **2018**, <https://dx.doi.org/10.26434/chemrxiv.7234721.v3>.
- [3] T. W. Ebbesen, *Acc. Chem. Res.* **2016**, *49*, 2403–2412.
- [4] a) B. S. Simpkins, K. P. Fears, W. J. Dressick, B. T. Spann, A. D. Dunkelberger, J. C. Owrutsky, *ACS Photonics* **2015**, *2*, 1460–1467; b) J. P. Long, B. S. Simpkins, *ACS Photonics* **2015**, *2*, 130–136; c) M. Muallem, A. Palatnik, G. D. Nessim, Y. R. Tischler, *J. Phys. Chem. Lett.* **2016**, *7*, 2002–2008.
- [5] a) J. Galego, C. Climent, F. J. Garcia-Vidal, J. Feist, *Phys. Rev. X* **2019**, *9*, 021057; b) J. Flick, M. Ruggenthaler, H. Appel, A. Rubio, *Proc. Natl. Acad. Sci. USA* **2017**, *114*, 3026–3034; c) H. L. Luk, J. Feist, J. J. Toppari, G. Groenhof, *J. Chem. Theory Comput.* **2017**, *13*, 4324–4335; d) J. Campos-Gonzalez-Angulo, R. F. Ribeiro, J. Yuen-Zhou, arXiv:1902.10264 [cond-mat, physics:physics, physics:quant-ph], **2019**.
- [6] R. M. A. Vergauwe, J. George, T. Chervy, J. A. Hutchison, A. Shalabney, V. Y. Torbeev, T. W. Ebbesen, *J. Phys. Chem. Lett.* **2016**, *7*, 4159–4164.
- [7] a) R. F. Ribeiro, L. A. Martínez-Martínez, M. Du, J. Campos-Gonzalez-Angulo, J. Yuen-Zhou, *Chem. Sci.* **2018**, *9*, 6325–6339; b) P. Törmä, W. L. Barnes, *Rep. Prog. Phys.* **2015**, *78*, 013901.
- [8] a) D. B. Northrop, *Acc. Chem. Res.* **2001**, *34*, 790–797; b) B. M. Dunn, *Chem. Rev.* **2002**, *102*, 4431–4458; c) K. S. Jin, Y. Rho, J. Kim, H. Kim, I. J. Kim, M. Ree, *J. Phys. Chem. B* **2008**, *112*, 15821–15827.
- [9] a) K. Liu, *Annu. Rev. Phys. Chem.* **2016**, *67*, 91–111; b) F. F. Crim, *Acc. Chem. Res.* **1999**, *32*, 877–884.
- [10] a) D. M. Coles, Y. Yang, Y. Wang, R. T. Grant, R. A. Taylor, S. K. Saikin, A. Aspuru-Guzik, D. G. Lidzey, J. K.-H. Tang, J. M. Smith, *Nat. Commun.* **2014**, *5*, 5561; b) D. M. Coles, L. C. Flatten, T. Sydney, E. Hounslow, S. K. Saikin, A. Aspuru-Guzik, V. Vedral, J. K.-H. Tang, R. A. Taylor, J. M. Smith, et al., *Small* **2017**, *13*, 1701777; c) C. P. Dietrich, A. Steude, L. Tropic, M. Schubert, N. M. Kronenberg, K. Ostermann, S. Höfling, M. C. Gather, *Sci. Adv.* **2016**, *2*, e1600666.
- [11] a) F. Perakis, L. De Marco, A. Shalit, F. Tang, Z. R. Kann, T. D. Kühne, R. Torre, M. Bonn, Y. Nagata, *Chem. Rev.* **2016**, *116*, 7590–7607; b) G. M. Hale, M. R. Querry, *Appl. Opt.* **1973**, *12*, 555–563; c) H. J. Bakker, J. L. Skinner, *Chem. Rev.* **2010**, *110*, 1498–1517.
- [12] D. Laage, T. Elsaesser, J. T. Hynes, *Chem. Rev.* **2017**, *117*, 10694–10725.
- [13] a) P. Ball, *Chem. Rev.* **2008**, *108*, 74–108; b) E. Brini, C. J. Fennell, M. Fernandez-Serra, B. Hribar-Lee, M. Lukšič, K. A. Dill, *Chem. Rev.* **2017**, *117*, 12385–12414.
- [14] a) M. Gruebele, K. Dave, S. Sukenik, *Annu. Rev. Biophys.* **2016**, *45*, 233–251; b) K. A. Dill, J. L. MacCallum, *Science* **2012**, *338*, 1042–1046; c) Y. Levy, J. N. Onuchic, *Annu. Rev. Biophys. Biomol. Struct.* **2006**, *35*, 389–415.
- [15] J. George, T. Chervy, A. Shalabney, E. Devaux, H. Hiura, C. Genet, T. W. Ebbesen, *Phys. Rev. Lett.* **2016**, *117*, 153601.
- [16] D. Meiser, P. Meystre, *Phys. Rev. A* **2006**, *74*, 065801.
- [17] M. Poreba, A. Szalek, W. Rut, P. Kasperkiewicz, I. Rutkowska-Włodarczyk, S. J. Snipas, Y. Itoh, D. Turk, B. Turk, C. M. Overall, et al., *Sci. Rep.* **2017**, *7*, 43135.
- [18] a) J.-J. Max, C. Chapados, *J. Phys. Chem. A* **2004**, *108*, 3324–3337; b) H. Li, X. Kong, L. Jiang, Z.-F. Liu, *Phys. Chem. Chem. Phys.* **2018**, *20*, 26918–26925.
- [19] a) A. Krzemińska, V. Moliner, K. Świderek, *J. Am. Chem. Soc.* **2016**, *138*, 16283–16298; b) T. J. Paul, A. Barman, M. Ozbil, R. P. Bora, T. Zhang, G. Sharma, Z. Hoffmann, R. Prabhakar, *Phys. Chem. Chem. Phys.* **2016**, *18*, 24790–24801.
- [20] a) T. Baumann, M. Hauf, F. Schildhauer, K. B. Eberl, P. M. Durkin, E. Deniz, J. G. Löffler, C. G. Acevedo-Rocha, J. Jaric, B. M. Martins, et al., *Angew. Chem. Int. Ed.* **2019**, *58*, 2899–2903; *Angew. Chem.* **2019**, *131*, 2925–2930; b) R. K. Harijan, I. Zoi, D. Antoniou, S. D. Schwartz, V. L. Schramm, *Proc. Natl. Acad. Sci. USA* **2018**, *115*, E6209–E6216.
- [21] a) J. Galego, C. Climent, F. J. Garcia-Vidal, J. Feist, *Phys. Rev. X* **2019**, *9*, 021057; b) F. Herrera, F. C. Spano, *Phys. Rev. Lett.* **2016**, *116*, 238301.

Manuscript received: July 16, 2019

Revised manuscript received: August 23, 2019

Accepted manuscript online: August 26, 2019

Version of record online: September 17, 2019